

Article

# Two Channels Opto-Isolation Circuit for Measurements of the Differential Voltage of Voltage Transformers and Dividers

Michał Kaczmarek 

Institute of Mechatronics and Information Systems, Lodz University of Technology, 90-924 Lodz, Poland; [michal.kaczmarek@p.lodz.pl](mailto:michal.kaczmarek@p.lodz.pl)

**Abstract:** In this paper the design of the two channel opto-isolation circuit for measurements of the differential voltage is presented. It is used to ensure high impedance of the measuring channel(s) in the differential system to ensure the rated operation of connected voltage divider(s). Its conversion accuracy tests are oriented to determine the ratio and phase errors introduced by a tested device under three test conditions. The opto-isolation circuit is tested for the internal noise at various levels of common voltage. In the next step the calibration of the zero output voltage at zero differential voltage is tested. In the last step of the testing procedure, the values of conversion ratio and phase errors are determined. In the first case the analysis is performed during an operation with an additional common voltage divider when both inputs ensure high impedance. In the second case the values of the conversion ratio and phase errors are tested in conditions when only one input ensures high impedance. In this paper the application of the opto-isolation circuit to determine the values of the composite error of the tested voltage divider with the rated voltage ratios equal to 15 kV:100 V, 10 kV:100 V, 5 kV:100 V is presented. Moreover, its usage to determine the values of the composite error of the inductive voltage transformer with voltage ratio  $(15 \text{ kV}/\sqrt{3})/(100 \text{ V}/\sqrt{3})$  is shown.

**Keywords:** opto-isolation; high impedance; distorted primary voltage; harmonics; voltage ratio error; phase displacement; voltage transformer; voltage divider



**Citation:** Kaczmarek, M. Two Channels Opto-Isolation Circuit for Measurements of the Differential Voltage of Voltage Transformers and Dividers. *Energies* **2022**, *15*, 2694. <https://doi.org/10.3390/en15072694>

Academic Editor: Adolfo Dannier

Received: 25 February 2022

Accepted: 1 April 2022

Published: 6 April 2022

**Publisher's Note:** MDPI stays neutral with regard to jurisdictional claims in published maps and institutional affiliations.



**Copyright:** © 2022 by the author. Licensee MDPI, Basel, Switzerland. This article is an open access article distributed under the terms and conditions of the Creative Commons Attribution (CC BY) license (<https://creativecommons.org/licenses/by/4.0/>).

## 1. Introduction

The presence of higher harmonics in the voltages of the power grid causes instrument transformers to be used to transform distorted voltage. Therefore, there is the necessity to test their transformation accuracy in increased frequency ranges [1–10]. Passive voltage dividers are widely used in testing the transformation accuracy of the instrument voltage transformers (VT) for distorted voltage. This is due to their linear frequency response unlike the resonance behavior of inductive VTs [11–18]. However, the resonance frequencies are far more different for various types of inductive VTs. Therefore, their testing of the transformation of the distorted voltage is required to indicate the wideband units. The developed device is used for measurements of the differential voltage and is required to ensure high impedance of the input connected to the passive voltage divider, where an additional load may lead to its inaccuracy and deterioration in the frequency response [12,14,17]. The differential voltage is used to determine the voltage composite error of the instrument voltage transformer [14,19]. Its values may be applied to determine the values of the voltage error and phase displacement for transformation of the distorted voltage harmonics to decrease the uncertainty of their evaluation in relation to the method when two voltages from the outputs of the tested and reference dividers are compared [20]. This cost effective solution is found to be efficient in testing transformation accuracy of the inductive voltage transformers for distorted voltage as presented in the papers [4,14,15,20].

In this paper a two channel opto-isolation circuit designed for measurements of the differential voltage between two passive voltage dividers or between a passive divider and an instrument voltage transformer is presented. The opto-isolation circuit in a single

channel is composed of high impedance ( $10^{12} \Omega$  DC) operational amplifiers for the channel input stage and output of the opto-coupling diode. The fast differential amplifier is used to compare the input voltages in relation to the common voltage obtained from the common voltage divider. The two channel opto-isolation circuit may be used for measurements of the differential voltage. The differential voltage maximum 5V RMS is measured between both inputs of the device at the level that does not exceed 200 V RMS. The tests are performed over two produced units. Two types of operation are presented in the examples section. If both channels are required to ensure high impedance, the additional voltage divider is required to obtain the floating reference voltage at a level not exceeding 5 V in relation to each input. In this configuration the device may be used to determine the differential voltage between two passive voltage dividers. If a single channel is required to ensure high impedance, one input is shorted with the common voltage input and connected to the tested VT, while the other input is connected to the reference voltage divider. The input used for the inductive VT does not require high impedance but it is still not less than 100 k  $\Omega$ . Both types of the application are presented in detail.

## 2. Conversion Accuracy Tests of the Two Channels Opto-Isolation Circuit

The conversion accuracy tests are oriented to determine the ratio and phase errors introduced by the tested device under three test conditions. The opto-isolation circuit is tested for the internal noise at various levels of common voltage. In this condition the inputs are shorted together while the common voltage is applied. In the next step the opto-isolation circuit calibration of the differential voltage zero is tested. Therefore, the inputs IN are shorted together, while different values of input and common voltages are applied to the IN inputs and COM input. In the last step of the testing procedure developed for the two channel opto-isolation circuit, the values of the conversion ratio and phase errors are tested. In the first case the analysis is performed during an operation with an additional common voltage divider when both inputs ensure high impedance. In the second case the values of the conversion ratio and phase errors are tested in conditions when only one input ensures high impedance because the other input is shorted with the common voltage input.

In Figure 1a the connections diagram of the two channel opto-isolation circuit during its conversion accuracy tests is presented. In Figure 1b the blocks diagram of the measuring setup for testing the two channel opto-isolation circuit is shown. In Figure 1c the photo of the measuring setup is presented.

In Figure 1a–c the following abbreviations are used:

OIC—opto-isolation circuit,

IC—internal circuit,

$IN_1/IN_2$ —differential voltage inputs of the OIC,

COM—common voltage input,

AWG—arbitrary waveform generator,

PA—power amplifier,

PS—power supply (PA + AWG) [21–23],

BPS—battery power supply,

$V_{diff}$ —differential input voltage measured by the DPM,

$V_{out}$ —output voltage of OIC measured by the DPM,

$V_{COM}$ —common voltage of the OIC inputs  $IN_1$  and  $IN_2$  measured by the voltmeter,

DPM—digital power meter,

$VD_1/VD_2/VD_{COM}$ —resistive–capacitive voltage divider,

$R_1/R_2/R_3$ —resistance of voltage dividers  $VD_1/VD_2/VD_{COM}$ ,

$R_{Var1}/R_{Var2}/R_{Var3}$ —variable resistance of voltage dividers  $VD_1/VD_2/VD_{COM}$ ,

$C_{Var1}/C_{Var2}/C_{Var3}$ —variable capacitance of voltage dividers  $VD_1/VD_2/VD_{COM}$ .

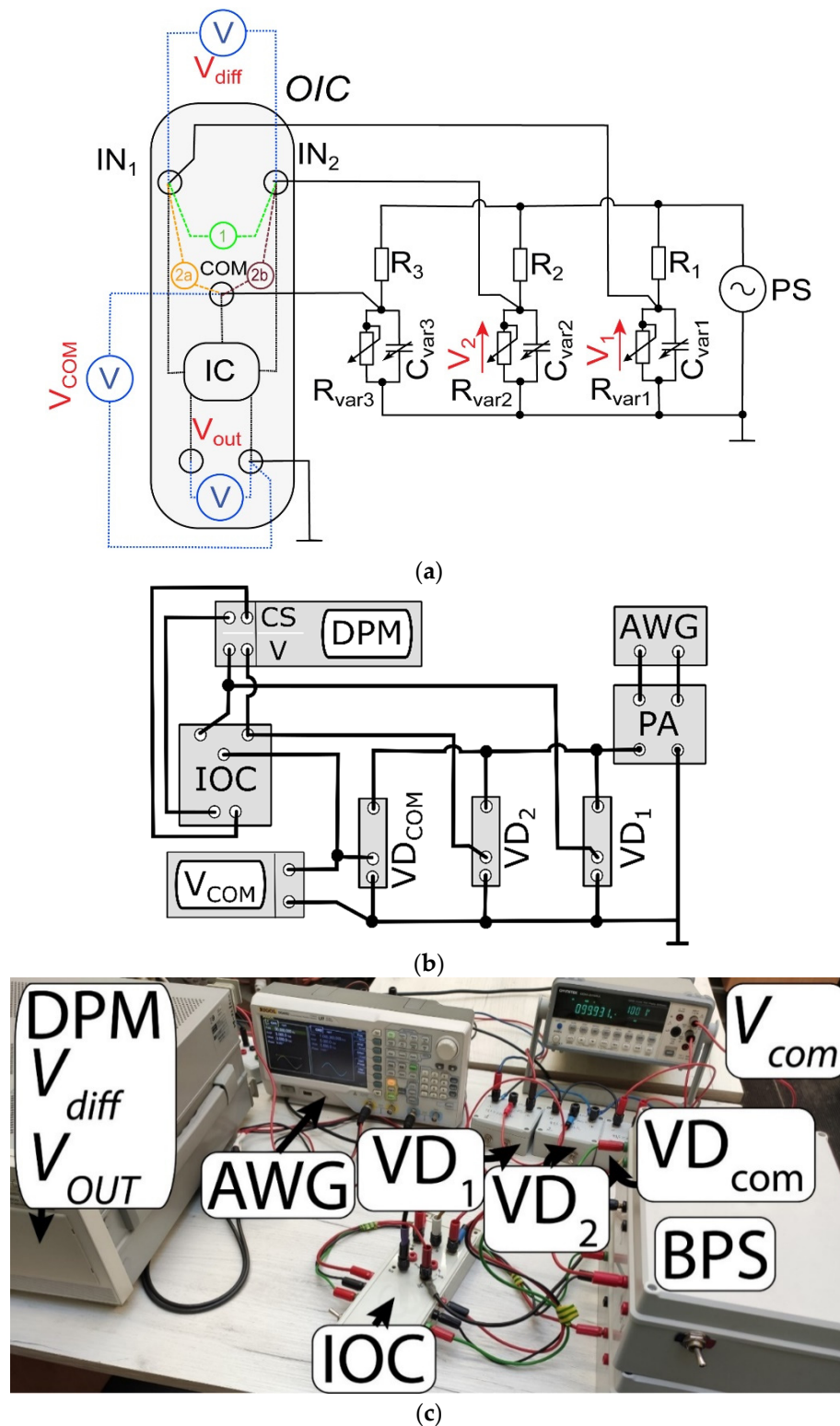


**Figure 1.** (a) Connections diagram of the two channel opto-isolation circuit during its tests. (b) Blocks diagram of the measuring setup for testing the two channel opto-isolation circuit. (c) Photo of the measuring setup for testing the two channel opto-isolation circuit.

Connection 1 presented in Figure 1a is used only during the conversion accuracy tests. Connection 2a or 2b is used to switch between the operational modes: with the additional common voltage divider (two inputs  $IN_1/IN_2$  ensure high impedance) or without this divider but only one input ensures high impedance.

The power supply is composed of the arbitrary waveform generator and the power amplifier. The values of  $R_{Var1}/R_{Var2}/R_{Var3}$  and  $C_{Var1}/C_{Var2}/C_{Var3}$  of the voltage dividers are set in order to ensure the required test values of common voltage (from 1 V to 200 V RMS) and differential voltage (0.1 V and 1 V RMS).

The conversion ratio error (presented in (%)) of transformation of the  $hk$ -order harmonic of the distorted voltage by the OIC is given by the equation

$$\Delta U_{hk} = \frac{V_{OUThk} - V_{diffhk}}{V_{diffhk}} \cdot 100\% \quad (1)$$

The conversion phase error (presented in ( $^{\circ}$ )) of transformation of the  $hk$ -order harmonic of the distorted voltage by the OIC is given by the equation

$$\delta \varphi_{hk} = \varphi_{V_{OUThk}} - \varphi_{V_{diffhk}} \quad (2)$$

$\varphi_{V_{diffhk}}$ —the phase angle of the  $hk$ -order harmonic in the input voltage of the OIC in relation to its main component,  $\varphi_{V_{OUThk}}$ —the phase angle of the  $hk$ -order harmonic of the output voltage of OIC in relation to the main harmonic of its input voltage.

In Figure 2 the internal diagram of the opto-isolation circuit designed to ensure high input impedance for measurements of the differential voltage is presented.

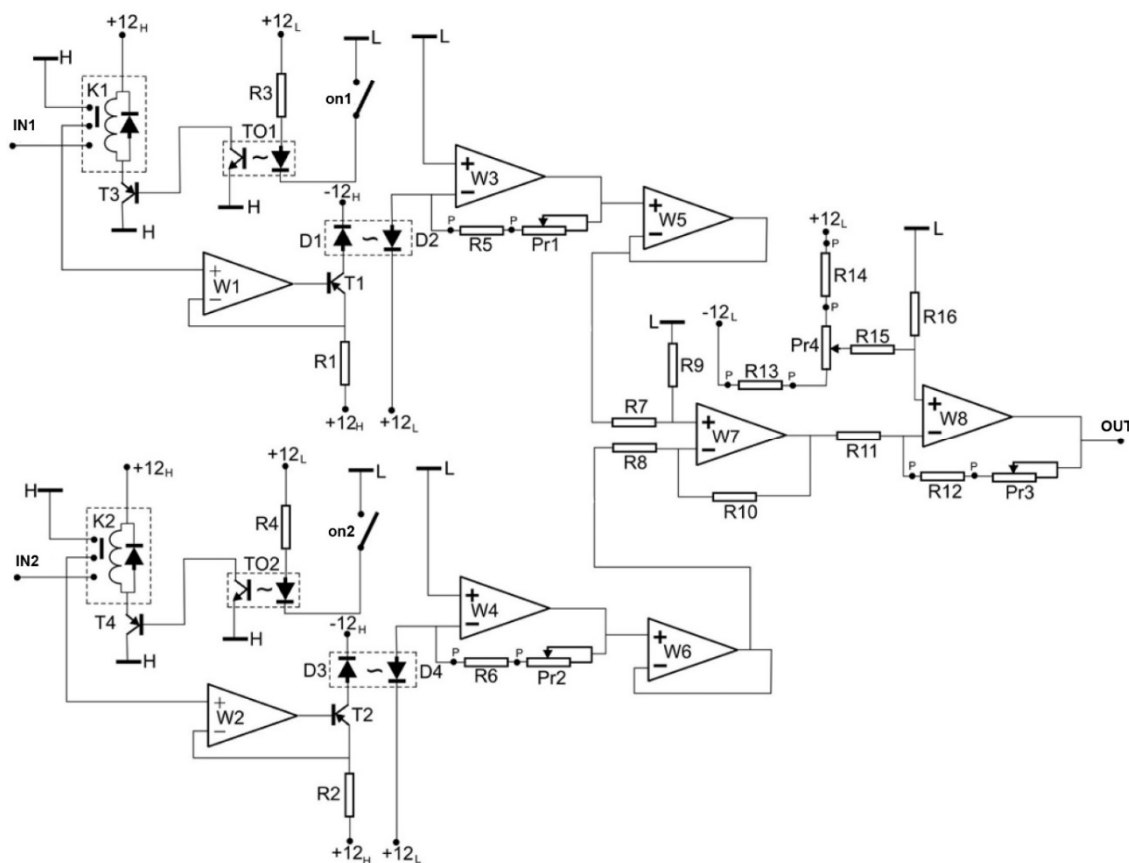


**Figure 2.** Internal diagram of the opto-isolation circuit designed to ensure high input impedance for measurements of the differential voltage.

In Figure 2 the following abbreviations are used:

- +/-12H—positive and negative high voltage side supply voltage,
- +/-12L—positive and negative low voltage side supply voltage,
- L—ground,

*H*—high voltage potential from common voltage divider,  
*K1/2*—reed relay for activation of inputs  $IN_{1/2}$ ,  
*TO1/2*—transoptors with above 1 kV separation voltage,  
*on1/2*—microswitch to activate the inputs by the transoptors,  
*D1/3*—transmitting diodes of the opto-coupler circuit,  
*D2/4*—receiving diodes of the opto-coupler circuit,  
*OUT*—output of the opto-isolation circuit,  
*W1:6*—high impedance ( $10^{12} \Omega$  DC) operational amplifiers,  
*W7/8*—fast differential amplifiers,  
*T1:4*—transistors,  
*R1:15*—resistors,  
*Pr1:4*—variable resistors.

The *W1* and *W2* amplifiers are powered by high voltage side power supply, other amplifiers are powered by the low voltage side power supply.

Transmitting and receiving diodes in pairs *D1* and *D2*, *D3* and *D4* are mounted in a 2.5 cm long tube.

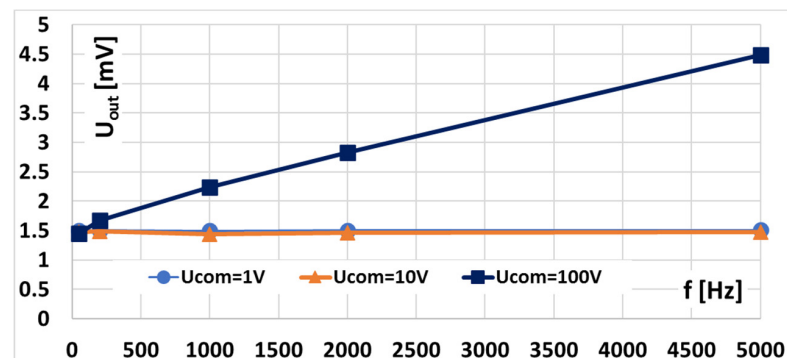
Resistors *R1* and *R2* are used to provide adequate power of the transmitting diode.

Resistors from *R8* to *R10* are used to set the zero offset of the differential operational amplifier *W7*.

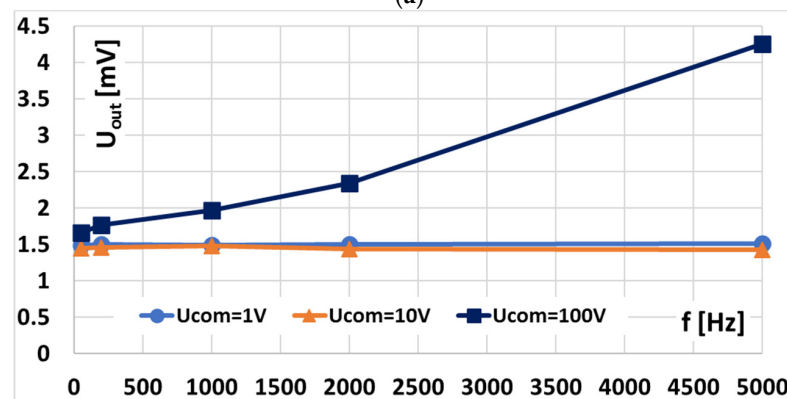
Resistors *R13*, *R14*, *R15*, *R16* and *Pr4* constitute the offset voltage compensation circuit.

Resistors *R11*, *R12* and *Pr3* set the gain of the entire path to the required value equal to 1.

In Figure 3a,b the results of the tests of the 1st and the 2nd units of the designed opto-isolation circuits performed to determine the RMS values of the internal noise for a given RMS value of the common voltage at frequency from 50 Hz to 5 kHz are presented.



(a)



(b)

**Figure 3.** (a) The 1st opto-isolation circuit tested to determine the RMS values of the internal noise for a given RMS value of the common voltage at frequency from 50 Hz to 5 kHz. (b) The 2nd opto-isolation circuit tested to determine the RMS values of the internal noise for a given RMS value of the common voltage at frequency from 50 Hz to 5 kHz.

The opto-isolation circuit is tested for the internal noise at various levels of common voltage and its frequency. In these conditions the differential inputs and the common voltage input are shorted together while the common voltage is applied. The output voltage is measured. In the ideal circuit the value should be equal to 0. The values of the output voltage are the same for both tested units. If the value of the common voltages are equal to 1 V or 10 V RMS, the output voltage is constant at level 1.5 mV RMS. If the value of the common voltage increases to 100 V RMS, the value of the output voltage increases with a frequency from 1.7 mV RMS for 50 Hz up to 5 mV RMS for 5 kHz. The measured value of the output voltage results not only from the different RMS values of the internal noise at each internal opto-isolation channel but also from its phase angle between the differential inputs of the internal operational amplifier W7.

In Figure 4a,b the results of the tests of the 1st and the 2nd units of the designed opto-isolation circuits performed to determine the calibration of the zero output voltage vs frequency of the differential input voltage at various levels of common voltage are presented.

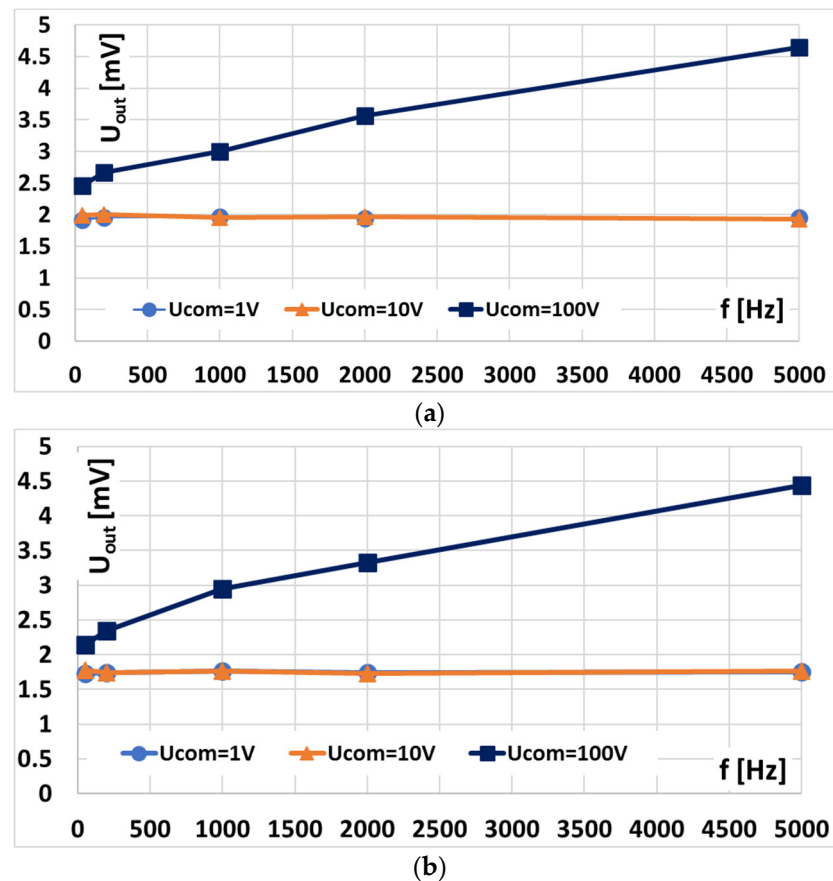


**Figure 4.** (a) The 1st opto-isolation circuit calibration of the zero output voltage vs frequency of the differential input voltage at various level of common voltage. (b) The 2nd opto-isolation circuit calibration of the zero output voltage vs frequency of the differential input voltage at various level of common voltage.

The opto-isolation circuit is tested for the calibration of the zero output voltage at various levels of common voltage and its frequency. In these conditions the differential inputs are shorted together while the common voltage and input voltage are applied. The output voltage is measured. In the ideal circuit the value should be still equal to 0 since the differential voltage is equal to 0. The values of the output voltage are similar for both tested units. If the values of the common voltages are equal to 1 V or 10 V RMS, the output voltage is constant at level 1.7 mV RMS or 2.0 mV RMS. If the value of the common voltage

increases to 100 V RMS, the value of the output voltage increases with a frequency from 2.2 mV RMS or 2.5 mV RMS for 50 Hz up to about 4.5 mV RMS for 5 kHz. The measured value of the output voltage in these conditions is similar to that obtained during the test of the internal noise. Therefore, the calibration of the zero value of the output voltage for zero value of the differential input voltage is performed correctly.

In Figure 5a,b the 1st and the 2nd opto-isolation circuits' conversion ratio errors under operation with an additional common voltage divider are presented.

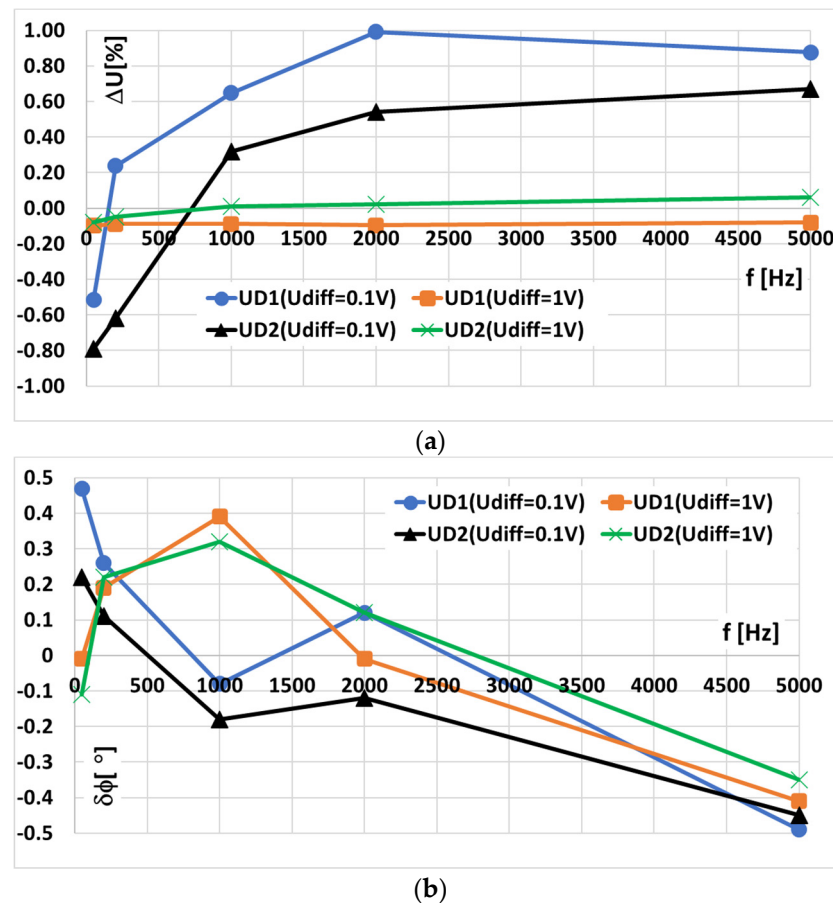
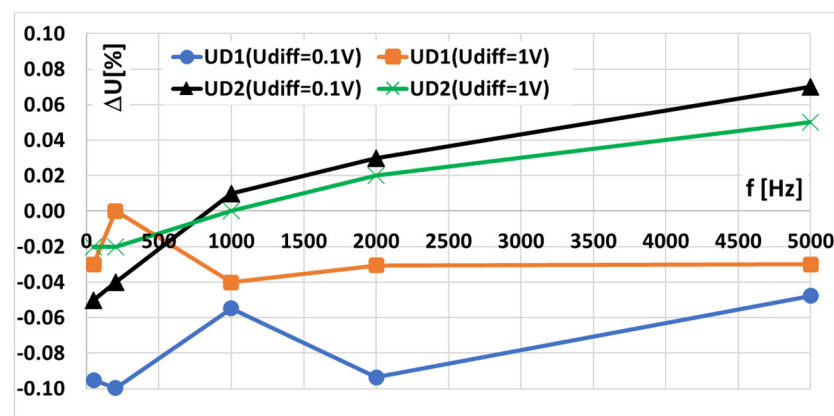


**Figure 5.** (a) The 1st and the 2nd opto-isolation circuits' conversion ratio errors under operation with an additional common voltage divider. (b) The 1st and the 2nd opto-isolation circuits' conversion phase error under operation with an additional common voltage divider.

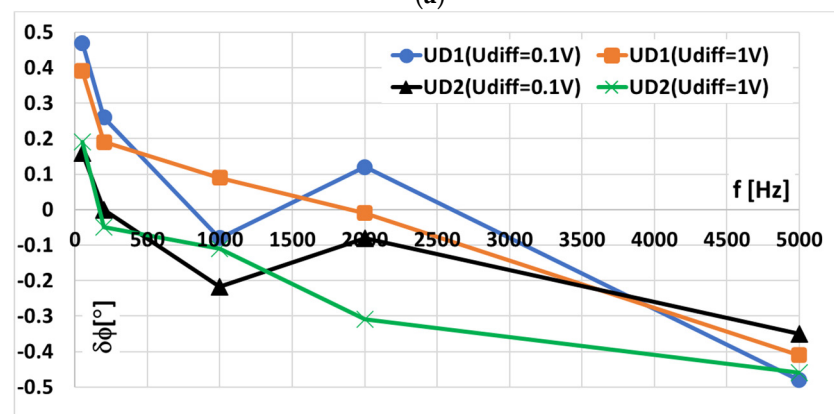
In these conditions in the measuring system from Figure 1, three voltage dividers are used. The output voltages of the  $VD1$  and the  $VD2$  are used to supply the differential input, while the  $VDCOM$  is used to supply the common voltage input. Therefore, the differential voltage between inputs  $IN_1$  and  $IN_2$  is measured in relation to the common voltage at input  $COM$ . Both input channels are insulated by the high impedance operational amplifiers and opto-isolation circuit of the coupling diodes.

The values of the opto-isolation circuits' conversion ratio errors are not exceeding  $\pm 1\%$ , while the value of the differential voltage is equal to 0.1 V RMS. Increases in the input voltage to 1 V RMS cause an increase in the accuracy of both tested units of the opto-isolation circuits to  $\pm 0.1\%$ . This is due to the fact that the opto-isolation circuits' conversion ratio errors result from the RMS value and phase shift of the internal noise between its internal input channels. The 1st and the 2nd opto-isolation circuits' conversion phase error under operation with an additional common voltage divider are not exceeding  $\pm 0.5^\circ$ , while the value of the differential voltage is equal to 0.1 V RMS and 1 V RMS.

In Figure 6a,b the 1st and the 2nd opto-isolation circuits' conversion ratio errors under operation without an additional common voltage divider are presented. If a single channel is required to ensure high impedance, one input is shorted with the common voltage input, while the other input is connected to the reference voltage divider. In these conditions in the measuring system from Figure 1, two voltage dividers are used. The output voltages of the  $VD_1$  are used to supply the differential input, while the  $VD_{COM}$  is used to supply the common voltage input. Therefore, the differential voltage between inputs  $IN_1$  and  $IN_2$  ( $COM$ ) is measured in relation to the common voltage at input  $IN_2$  ( $COM$ ). Only the  $IN_1$  input channel is insulated by the high impedance operational amplifiers and opto-isolation circuit of the coupling diodes.



(a)



(b)

**Figure 6.** (a) The 1st and the 2nd opto-isolation circuits' conversion ratio error under operation without an additional common voltage divider (input  $IN_2$  shorted with common voltage input). (b) The 1st and the 2nd opto-isolation circuits' conversion phase error under operation without an additional common voltage divider (input  $IN_2$  shorted with common voltage input).

The values of the opto-isolation circuits' conversion ratio errors are not exceeding  $\pm 0.1\%$ , while the value of the differential voltage is equal to 0.1 V RMS and 1 V RMS. This is due to the fact that the opto-isolation circuits' conversion ratio errors result from the RMS value of the internal noise of the single internal input channel. The 1st and the 2nd opto-isolation circuits' conversion phase error under operation with an additional common voltage divider are not exceeding  $\pm 0.5^\circ$ , while the value of the differential voltage is equal to 0.1 V RMS and 1 V RMS.

### 3. Applications of the Two Channel Opto-Isolation Circuit

In this paragraph of the paper, the application of the opto-isolation circuit to determine the values of the composite error of the tested voltage divider with the rated voltage ratios

equal to 15 kV:100 V, 10 kV:100 V, 5 kV:100 V is presented. The opto-isolation circuit operates with an additional common voltage divider connected to the input COM. The input  $IN_1$  is connected to the high potential terminal of the output of the reference voltage divider. The input  $IN_2$  is connected to the high potential terminal of the tested voltage divider (Figure 7).

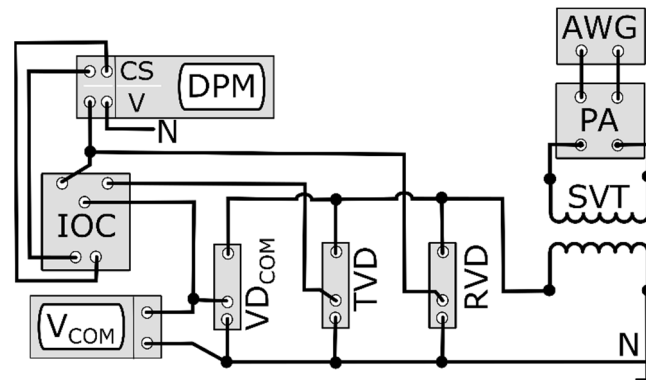


**Figure 7.** Blocks diagram of the measuring setup for the application of the opto-isolation circuit to determine the values of the composite error of the voltage divider.

In Figure 7 the same abbreviations as in Figure 1 are used and additionally:

SVT—step-up voltage transformer [20],

TVD—tested voltage divider,

RVD—reference voltage divider,

CS—current sense channel of DPM (voltage input designed to connect current probe),

V—voltage channel of DPM.

In Figure 7 the opto-isolation circuit (OIC) is used to determine the values of the composite error of the tested voltage divider (TVD) in relation to the reference voltage divider (RVD).

The composite error of transformation of the  $hk$ -order harmonic of the distorted voltage  $\Delta\varepsilon_{TV Dhk}$  by the TVD is calculated from the equation

$$\Delta\varepsilon_{TV Dhk} = \frac{U_{OIC hk}}{U_{RVD hk}} \cdot 100\% \quad (3)$$

$U_{RVD hk}$ —the RMS values of a given harmonic in the output voltage of the RVD,

$U_{OIC hk}$ —the RMS values of a given higher harmonic in the output voltage of the OIC.

In accordance with analysis presented in papers [14,15,19,20], to decrease the measurement uncertainty of values of voltage ratio error and phase displacement, a  $hk$  harmonic of the output voltage  $U_{TV Dhk}$  of TVD may be calculated from the differential voltage measured by the OIC.

$$U_{TV Dhk} = \sqrt{U_{RVD hk}^2 + U_{OIC hk}^2 - 2 \cdot U_{RVD hk} \cdot U_{OIC hk} \cdot \cos(180 - \varphi_{RVDOIC hk})} \quad (4)$$

$\varphi_{RVDOIC}$ —the phase angle of a given harmonic in the output voltage of the OIC in relation to the same frequency harmonic in the reference voltage from the RVD.

The voltage ratio error (presented in (%)) of transformation of the  $hk$ -order harmonic of the distorted voltage by TVD is given by the equation

$$\Delta U_{TV Dhk} = \frac{U_{TV Dhk} - U_{RVD hk}}{U_{RVD hk}} \cdot 100\% \quad (5)$$

The phase displacement (presented in (°)) of transformation of the  $hk$ -order harmonic of the distorted voltage by  $TVD$  is given by the equation

$$\delta U_{TVD} = \arcsin\left(\frac{\sqrt{\Delta \varepsilon_{TVDhk}^2 - \Delta U_{TVDkh}^2}}{100\%}\right) \tag{6}$$

In Figure 8a,b the determined values of the voltage ratio error and phase displacement of the tested voltage divider at three ranges are presented.

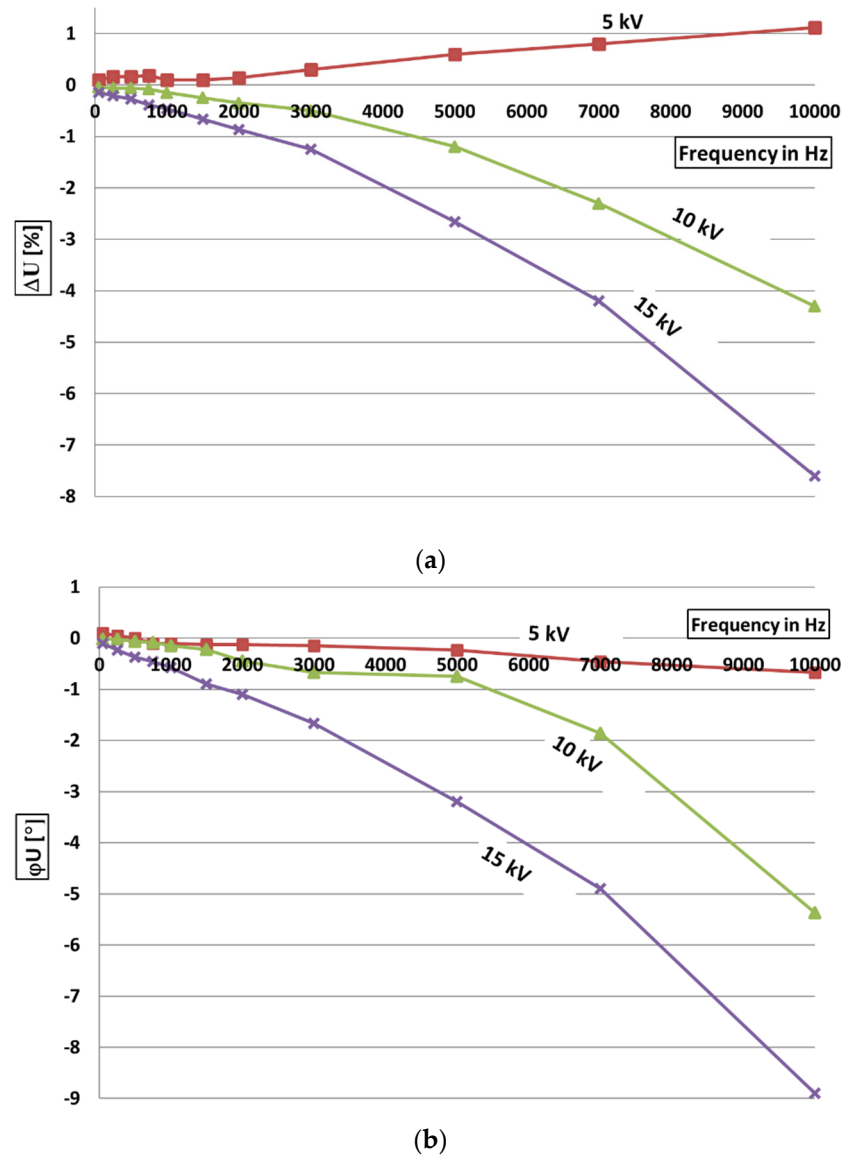


**Figure 8.** (a) Voltage ratio error of tested voltage divider at three ranges. (b) Phase error of tested voltage divider at three ranges.

The result of the measurements show that at the range 15 kV:100 V of  $TVD$  the values of voltage ratio error and phase displacement did not exceed  $\pm 8\%$  and  $\pm 9^\circ$ , respectively. The result indicates that at the range 10 kV:100 V the values of voltage ratio error and phase displacement did not exceed  $\pm 5\%$  and  $\pm 6^\circ$ , respectively, while, at the range 5 kV:100 V the values of voltage ratio error and phase displacement did not exceed  $\pm 1.5\%$  and  $\pm 1^\circ$ , respectively. The advantage of the application of  $OIC$  in testing the VDs is that it always ensure lower values of the measurement uncertainty than typical two channel systems, where reference voltage and output voltage of the tested VD are compared. The increase

in the frequency of the measured voltage results in more significant differences between the measurement uncertainties, showing a higher advantage of the differential method. The measurement uncertainties of the voltage ratio error and phase displacement for two harmonics of frequency 50 Hz and 5 kHz, and their values 5.0% and  $5.0^\circ$ , are equal to [20]:

- 50 Hz:  $\pm 0.507\% / \pm 0.535^\circ$ ;
- 5 kHz:  $\pm 0.178\% / \pm 2.160^\circ$ .

The expanded combined measurement uncertainty for 5 kHz is about three-fold lower than for 50 Hz because the measured value of the voltage's main component at the output of the RVD is ten-fold higher than the higher harmonic.

If the differential system is used with the designed OIC, the expanded combined measurement uncertainties of the values of ratio error and phase displacement are equal to [20]:

- 50 Hz:  $\pm 0.015\% / \pm 0.013^\circ$ ;
- 5 kHz:  $\pm 0.071\% / \pm 0.137^\circ$ .

Therefore, the application of OIC to determine the values of the voltage ratio error and phase displacement for the transformation of distorted voltage harmonics enables decreases in the measurement uncertainty.

In the next paragraph the application of the opto-isolation circuit (OIC) to determine the values of the composite error of the inductive VT with a voltage ratio equal to  $(15 \text{ kV} / \sqrt{3}) / (100 \text{ V} / \sqrt{3})$  is presented. The OIC operates without an additional common voltage divider. The input  $IN_1$  is connected to the high potential terminal of the output of the reference voltage divider with voltage ratio equal to  $15 \text{ kV} / 100 \text{ V}$ . The input  $IN_2$  is shorted with the common voltage input where the high potential terminal of the tested VT secondary winding is connected. The blocks diagram of the measuring setup is presented in Figure 9.

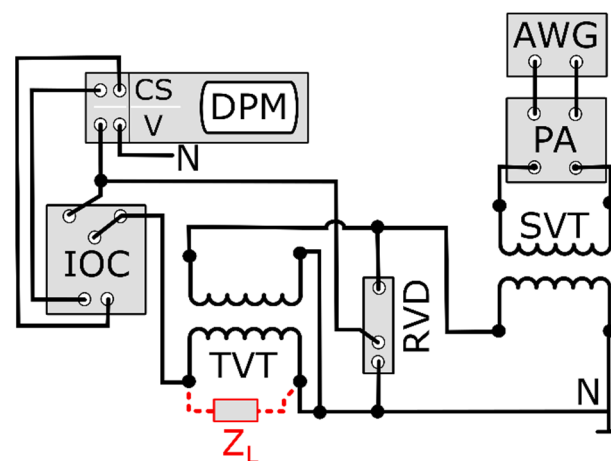


**Figure 9.** Blocks diagram of the measuring setup for the application of the opto-isolation circuit to determine the values of the composite error of the inductive VT.

In Figure 9 the same abbreviations as in Figures 1 and 7 are used and additionally:

TVT—tested voltage transformer,

$Z_L$ —load impedance of TVT (if required for test).

The composite error of transformation of the  $hk$ -order harmonic of the distorted voltage by the TVT  $\Delta\varepsilon_{TVThk}$  is calculated from the equation

$$\Delta\varepsilon_{TVThk} = \frac{U_{OIChk}}{U_{RVDhk}} \cdot 100\% \quad (7)$$

The  $hk$  harmonic of the secondary voltage of TVT  $U_{TVThk}$  may be calculated from the differential voltage measured by the OIC.

$$U_{TVThk} = \sqrt{U_{RVDhk}^2 + U_{OICHk}^2 - 2 \cdot U_{RVDhk} \cdot U_{OICHk} \cdot \cos(180 - \varphi_{RVDOICHk})} \quad (8)$$

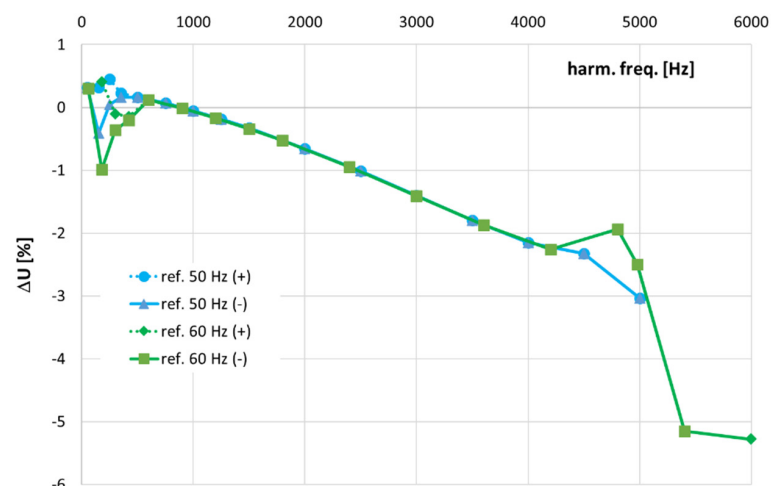
The voltage ratio error of transformation of the  $hk$ -order harmonic of the distorted voltage by TVT is given by the equation

$$\Delta U_{TVThk} = \frac{U_{TVThk} - U_{RVDhk}}{U_{RVDhk}} \cdot 100\% \quad (9)$$

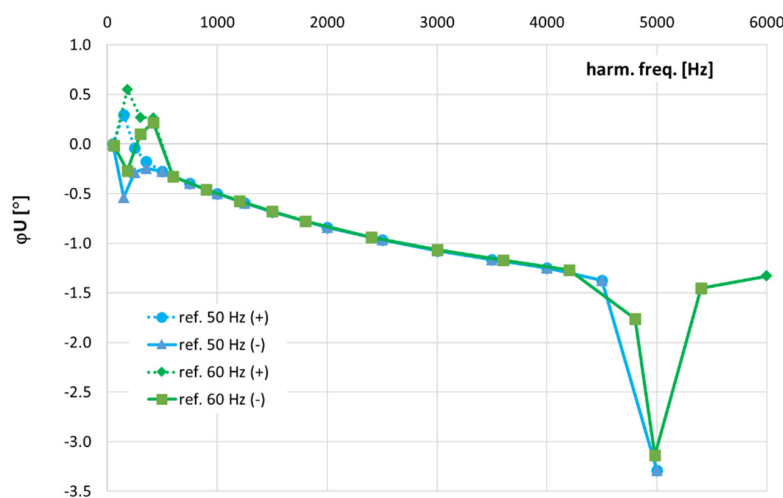
The phase displacement of transformation of the  $hk$ -order harmonic of the distorted voltage by TVT is given by the equation

$$\delta U_{TVT} = \arcsin\left(\frac{\sqrt{\Delta \varepsilon_{TVThk}^2 - \Delta U_{TVThk}^2}}{100\%}\right) \quad (10)$$

In Figure 10a,b the determined values of the voltage ratio error and phase displacement of the tested voltage transformer (15 kV/ $\sqrt{3}$ )/(100 V/ $\sqrt{3}$ ) are presented.



(a)



(b)

**Figure 10.** (a) The values of voltage ratio error of tested inductive VT. (b) The values of phase displacement of tested inductive VT.

In Figure 10 the following abbreviations are used

“50 Hz (+)” and “50 Hz (–)”—these plots present the results of the VT’s transformation accuracy of a given harmonic with the main component of frequency 50 Hz.

“60 Hz (+)” and “60 Hz (–)”—these plots present the results of the VT’s transformation accuracy of a given harmonic with the main component of frequency 60 Hz.

(+)—this notation means that the maximum positive values of voltage error and phase displacement are determined

(–)—this notation means that the maximum negative values of voltage error and phase displacement are determined.

The difference between the maximum positive values and the maximum negative values of voltage error and phase displacement results from the nonlinear of the B(H) curve of the tested inductive VT magnetic core and the self-generation of low-order higher harmonics to its secondary voltage [4,20,24,25]. Therefore, these curves are different only for the low-order higher harmonics up to about 500 Hz. The results of the measurements show that the values of the voltage ratio error and phase displacement of TVT did not exceed  $\pm 6\%$  and  $\pm 3.5^\circ$ , respectively. These values significantly increase with the frequency of transformed higher harmonics. This is caused by the increase in the reactance of the winding of TVT and the increase in their voltage. At a frequency of about 5 kHz, a resonance is detected causing a rapid increase in the VT’s voltage error and phase displacement [26–28].

If the differential system with the designed OIC is used, or a typical two channel system where output voltages of TVT and RVD are measured, the expanded combined measurement uncertainties of the values of ratio error and phase displacement are equal to those determined for TVD in the previous analyzed case. The advantage of the application of OIC in testing the VTs is still that it ensures lower values of the measurement uncertainty than the two channel system.

#### 4. Conclusions

The designed opto-isolation circuit is tested for the internal noise at various levels of common voltage and its frequency. The values of the output voltage are the same for both tested units. If the value of the common voltages are equal to 1 V or 10 V RMS, the output voltage is constant at level 1.5 mV RMS. If the value of the common voltage increases to 100 V RMS, the value of the output voltage increases with a frequency from 1.7 mV RMS for 50 Hz up to 5 mV RMS for 5 kHz. The opto-isolation circuit is also tested for the calibration of the zero output voltage at various level of common voltage and its frequency. The values of the output voltage are similar for both tested units. If the value of the common voltages are equal to 1 V or 10 V RMS, the output voltage is constant at level 1.7 mV RMS or 2.0 mV RMS. If the value of the common voltage increases to 100 V RMS, the value of the output voltage increases with a frequency from 2.2 mV RMS or 2.5 mV RMS for 50 Hz up to about 4.5 mV RMS for 5 kHz. The measured value of the output voltage in this conditions is similar to that obtained during the test of the internal noise. Therefore, the calibration of the zero value of the output voltage for the zero value of the differential input voltage is performed correctly. The values of the opto-isolation circuits’ conversion ratio errors do not exceed  $\pm 1\%$ , while the value of the differential voltage is equal to 0.1 V RMS. An increase in the input voltage to 1 V RMS causes an increase in the accuracy of both tested units of the opto-isolation circuits to  $\pm 0.1\%$ , regardless of the level of the common voltage. This is due to the fact that the opto-isolation circuits’ conversion ratio errors result from the RMS value and phase shift of the internal noise between its internal input channels. The 1st and 2nd opto-isolation circuits’ conversion phase error under operation with an additional common voltage divider do not exceed  $\pm 0.5^\circ$ , while the value of the differential voltage is equal to 0.1 V RMS and 1 V RMS.

The tests are performed over two produced units. Two types of operation are presented in the examples section. If both channels are required to ensure high impedance, an additional voltage divider is required to obtain the floating reference voltage at a level not exceeding 5 V in relation to each input. In this configuration the device may be used

to determine the differential voltage between two passive voltage dividers. If a single channel is required to ensure high impedance, one input is shorted with the common voltage input and connected to the tested VT, while the other input is connected to the reference voltage divider. In order to decrease the measurement uncertainty of the values of voltage ratio error and phase displacement, a hk harmonic of the output voltage of the tested voltage divider or tested voltage transformer may be calculated from the differential voltage measured by the designed opto-isolation circuit. The advantage of its application in testing voltage transformers and dividers is that it always ensures lower values of the measurement uncertainty than the typical two channel system, where reference voltage and output/secondary voltage are compared.

**Funding:** This research received no external funding.

**Institutional Review Board Statement:** Not applicable.

**Informed Consent Statement:** Not applicable.

**Data Availability Statement:** Not applicable.

**Conflicts of Interest:** The author declares no conflict of interest.

## References

1. IEC TR 61869-103:2012; Instrument Transformers—The Use of Instrument Transformers for Power Quality Measurement. IEC: Geneva, Switzerland, 2012.
2. IEC 61869-6:2016; Instrument Transformers—Part 6: Additional General Requirements for Low-Power Instrument Transformers. IEC: Geneva, Switzerland, 2016.
3. Faifer, M.; Laurano, C.; Ottoboni, R.; Toscani, S.; Zanoni, M.; Crotti, G.; Giordano, D.; Barbieri, L.; Gondola, M.; Mazza, P. Overcoming Frequency Response Measurements of Voltage Transformers: An Approach Based on Quasi-Sinusoidal Volterra Models. *IEEE Trans. Instrum. Meas.* **2019**, *68*, 2800–2807. [\[CrossRef\]](#)
4. Kaczmarek, M.; Stano, E. Why Should We Test the Wideband Transformation Accuracy of Medium Voltage Inductive Voltage Transformers? *Energies* **2021**, *14*, 4432. [\[CrossRef\]](#)
5. Elphick, S.; Gosbell, V.; Smith, V.; Perera, S.; Ciuffo, P.; Drury, G. Methods for Harmonic Analysis and Reporting in Future Grid Applications. *IEEE Trans. Power Deliv.* **2017**, *32*, 989–995. [\[CrossRef\]](#)
6. Dirik, H.; Duran, I.U.; Gezeğin, C. A Computation and Metering Method for Harmonic Emissions of Individual Consumers. *IEEE Trans. Instrum. Meas.* **2019**, *68*, 412–420. [\[CrossRef\]](#)
7. Buchhagen, C.; Fischer, M.; Hofmann, L.; Daumling, H. Metrological determination of the frequency response of inductive voltage transformers up to 20 kHz. In Proceedings of the 2013 IEEE Power & Energy Society General Meeting, Vancouver, BC, Canada, 21–25 July 2013. [\[CrossRef\]](#)
8. Faifer, M.; Laurano, C.; Ottoboni, R.; Toscani, S.; Zanoni, M. Harmonic Distortion Compensation in Voltage Transformers for Improved Power Quality Measurements. *IEEE Trans. Instrum. Meas.* **2019**, *68*, 3823–3830. [\[CrossRef\]](#)
9. Filipović-Grčić, D.; Filipović-Grčić, B.; Krajtner, D. Frequency response and harmonic distortion testing of inductive voltage transformer used for power quality measurements. *Procedia Eng.* **2017**, *202*, 159–167. [\[CrossRef\]](#)
10. Crotti, G.; Gallo, D.; Giordano, D.; Landi, C.; Luiso, M.; Modarres, M. Frequency response of MV voltage transformer under actual waveforms. *IEEE Trans. Instrum. Meas.* **2017**, *66*, 1146–1154. [\[CrossRef\]](#)
11. Rydler, K.; Svensson, S.; Tarasso, V. Voltage dividers with low phase angle errors for a wideband power measuring system. In Proceedings of the Conference Digest Conference on Precision Electromagnetic Measurements, Ottawa, ON, Canada, 16–21 June 2002; pp. 382–383.
12. Zucca, M.; Modarres, M.; Giordano, D.; Crotti, G. Accurate Numerical Modelling of MV and HV Resistive Dividers. *IEEE Trans. Power Deliv.* **2017**, *32*, 1645–1652. [\[CrossRef\]](#)
13. Garnacho, F.; Khamlichi, A.; Rovira, J. The design and characterization of a prototype wideband voltage sensor based on a resistive divider. *Sensors* **2017**, *17*, 2657. [\[CrossRef\]](#)
14. Kaczmarek, M. Development and application of the differential voltage to single-ended voltage converter to determine the composite error of voltage transformers and dividers for transformation of sinusoidal and distorted voltages. *Meas. J. Int. Meas. Confed.* **2017**, *101*, 53–61. [\[CrossRef\]](#)
15. Kaczmarek, M.; Szatilo, T. Reference voltage divider designed to operate with oscilloscope to enable determination of ratio error and phase displacement frequency characteristics of MV voltage transformers. *Meas. J. Int. Meas. Confed.* **2015**, *68*, 22–31. [\[CrossRef\]](#)
16. Crotti, G.; Gallo, D.; Giordano, D.; Landi, C.; Luiso, M. Medium voltage divider coupled with an analog optical transmission system. *IEEE Trans. Instrum. Meas.* **2014**, *63*, 2349–2357. [\[CrossRef\]](#)

17. Kaczmarek, M. The effect of distorted input voltage harmonics rms values on the frequency characteristics of ratio error and phase displacement of a wideband voltage divider. *Electr. Power Syst. Res.* **2019**, *167*, 1–8. [[CrossRef](#)]
18. IEC 61869-11:2017; Instrument Transformers—Part 11: Additional Requirements for Low Power Passive Voltage Transformers. IEC: Geneva, Switzerland, 2017.
19. Kaczmarek, M.; Stano, E. Proposal for extension of routine tests of the inductive current transformers to evaluation of transformation accuracy of higher harmonics. *Int. J. Electr. Power Energy Syst.* **2019**, *113*, 842–849. [[CrossRef](#)]
20. Kaczmarek, M.; Stano, E. Measuring system for testing the transformation accuracy of harmonics of distorted voltage by medium voltage instrument transformers. *Measurement* **2021**, *181*, 109628. [[CrossRef](#)]
21. Brodecki, D.; Stano, E.; Andrychowicz, M.; Kaczmarek, P. Emc of wideband power sources. *Energies* **2021**, *14*, 1457. [[CrossRef](#)]
22. Kaczmarek, M.L.; Stano, E. Application of the inductive high current testing transformer for supplying of the measuring circuit with distorted current. *IET Electr. Power Appl.* **2019**, *13*, 1310–1317. [[CrossRef](#)]
23. Kaczmarek, M.; Kaczmarek, P. Comparison of the wideband power sources used to supply step-up current transformers for generation of distorted currents. *Energies* **2020**, *13*, 1849. [[CrossRef](#)]
24. Kaczmarek, M.; Stano, E. Nonlinearity of Magnetic Core in Evaluation of Current and Phase Errors of Transformation of Higher Harmonics of Distorted Current by Inductive Current Transformers. *IEEE Access.* **2020**, *8*, 118885–118898. [[CrossRef](#)]
25. Stano, E.; Kaczmarek, M. Wideband self-calibration method of inductive cts and verification of determined values of current and phase errors at harmonics for transformation of distorted current. *Sensors* **2020**, *20*, 2167. [[CrossRef](#)]
26. Kaczmarek, M.; Brodecki, D. Transformation of Transient Overvoltages by Inductive Voltage Transformers. *Sensors* **2021**, *21*, 4167. [[CrossRef](#)] [[PubMed](#)]
27. Popov, M. General approach for accurate resonance analysis in transformer windings. *Electr. Power Syst. Res.* **2018**, *161*, 45–51. [[CrossRef](#)]
28. Kaczmarek, M.; Stano, E. Application of the Sinusoidal Voltage for Detection of the Resonance in Inductive Voltage Transformers. *Energies* **2021**, *14*, 7047. [[CrossRef](#)]